

Generalized two-fluid equilibria: Understanding RT-1 experiments and beyond

Z. Yoshida,¹ S. M. Mahajan,² T. Mizushima,¹ Y. Yano,¹ H. Saitoh,¹ and J. Morikawa¹

¹Graduate School of Frontier Sciences, The University of Tokyo, Kashiwa, Chiba 277-8561, Japan

²Institute for Fusion Studies, The University of Texas at Austin, Austin, Texas 78712, USA

(Received 16 June 2010; accepted 5 October 2010; published online 15 November 2010)

Diversity of plasma structures, which degenerates in the ideal magnetohydrodynamic model, can emerge in many ways in a two-fluid plasma endowed with a hierarchy of scales. We study the equilibrium structure of high-beta (high temperature and low-density) electrons in a relatively weak magnetic field. Spontaneous flow generation and strong diamagnetism are clear manifestations of the nonideal two-fluid dynamics scaled, respectively, by the ion and electron-inertia lengths (skin depths). The theory predicts stronger flow and diamagnetism in the nonlinear regime of the two-fluid dynamics. © 2010 American Institute of Physics. [doi:10.1063/1.3505821]

I. INTRODUCTION

The scale invariant ideal magnetohydrodynamic (MHD) model cannot capture the richness of the structures built around various physical scales (gyroradii, inertial lengths, or skin depths associated with different plasma constituents) present in a plasma. Unlike a neutral fluid for which only the collisional viscosity, by introducing an intrinsic scale (the Kolmogorov scale), breaks the scale invariance of the ideal fluid model, the scale invariance of a plasma may be broken by a variety of nondissipative yet nonideal effects. The consequential “nonideal” dynamics can be replete with structures reflecting a possible hierarchy of the intrinsic scales.

The unified form of matter and electromagnetic field coupling, formulated and described in Ref. 1, delineates how the effective forces enter plasma dynamics (to be reviewed in Sec. II). Mathematically, such nonideal scale-specific effects appear as *singular perturbations*; the equations of motion will contain a higher-order derivative term multiplied by a small coefficient.²

The aim of this paper is to examine, theoretically as well as experimentally, the scale dependent generalizations (generally referred to as *two-fluid effects*) of the simplest MHD models. In particular, we will examine the accessible equilibrium structures in the hierarchy of scales furnished by ion-inertia and electron-inertia; the physical parameters of the plasma may make either of the scales as the determinant of the structure.

Recent experiment on the RT-1 device (see Fig. 1) sheds light on these regimes of plasma confinement.³ Spontaneous flow generation and strong diamagnetism (confinement of very high-beta plasma) are clear manifestations of these nonideal effects. Observations pertaining to the present work are summarized as follows (see also the observations on a similar-geometry device LDX):⁴

(1) *Low-density operation.* The RT-1 device can operate at relatively low-density $n_0 \lesssim 10^{17} \text{ m}^{-3}$ (see Fig. 2). The corresponding ion-inertia length Δ_i is of the order of 1 m, while the length scale L_0 of the equilibrium structure (scaling the gradient in the pressure or magnetic field) is

0.05–0.2 m. The plasma is then freed from the ideal MHD constraints, leading to a “decoupling” of the ion and electron fluids.

- (2) *Hot electrons.* On RT-1, electrons are heated by ECH up to $T_e = 10\text{--}30 \text{ keV}$, producing very high-beta values (see Fig. 2). However, ions are left cold ($T_i \lesssim 10 \text{ eV}$), because no direct heating is applied for ions and the collisional heat transfer from very hot and low-density electrons is very small. The molar enthalpy (enthalpy per particle) of electrons is estimated to be $h_e \lesssim 10^{-14} \text{ J}$. Confinement of such a large thermal energy produces a strong diamagnetism.
- (3) *Electric potential and ion flow.* Near the boundary, the plasma is negatively charged ($\phi \approx -10 \text{ to } -20 \text{ V}$). The potential gradient changes sign deep inside the plasma (though inside probe measurement is limited to low temperature operations); see Fig. 3. We observe spontaneous ion flow with a speed $V_i \lesssim 10^4 \text{ m/s}$ in the ion diamagnetic direction; see Fig. 4.

These experimental results require, at least, a two-fluid theory to interpret the basic properties. The rest of the paper is organized as follows. In Sec. II, we display the basic equations of the two-fluid (electron-ion) plasma in a succinct unified form.¹ By normalizing variables, we delineate the scale hierarchy dictated by the relation among the cyclotron and plasma frequencies of both electrons and ions. In Sec. III, we study the aspects of dynamics that are dominated by the ion-inertia scale and discuss the spontaneous ion flow. Section IV is devoted to investigating the physics pertinent to scales set by the electron-inertia regime. Electron-inertia dictates the plasma edge region and turns out to be a source of strong diamagnetism.

II. TWO-FLUID EQUILIBRIA

A. Two-fluid model and Bernoulli–Beltrami conditions

For simplicity, we consider a quasineutral plasma with singly charged ions. The ions (with charge $q_i = e$ and mass m_i) and electrons (with charge $q_e = -e$ and mass m_e) have the same density n . Introducing *generalized electromagnetic*

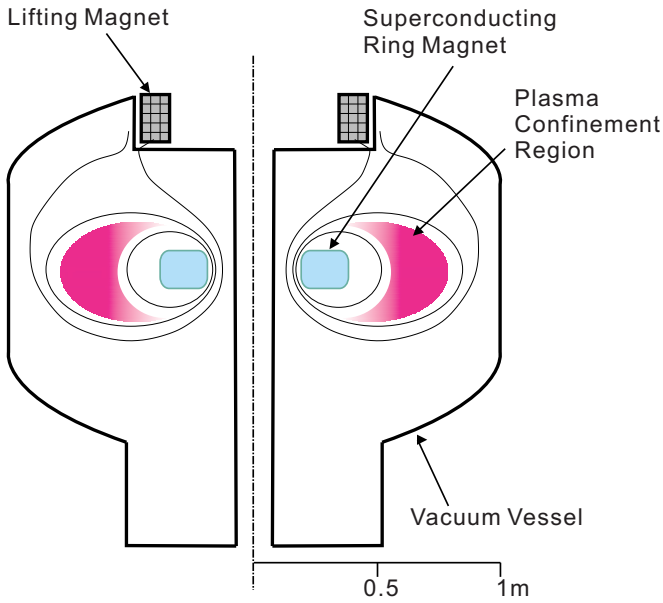


FIG. 1. (Color online) Schematic illustration of the RT-1 device. A dipole magnetic field is produced by the levitating superconducting ring magnet. The field strength in the confinement region varies from 0.5 to 0.01 T.

fields (we mark them by “tilde;” these fields must be distinguished from the later introduced *normalized variables* denoted by “hat” and “check”), the equation of motion for the species j can be written as¹

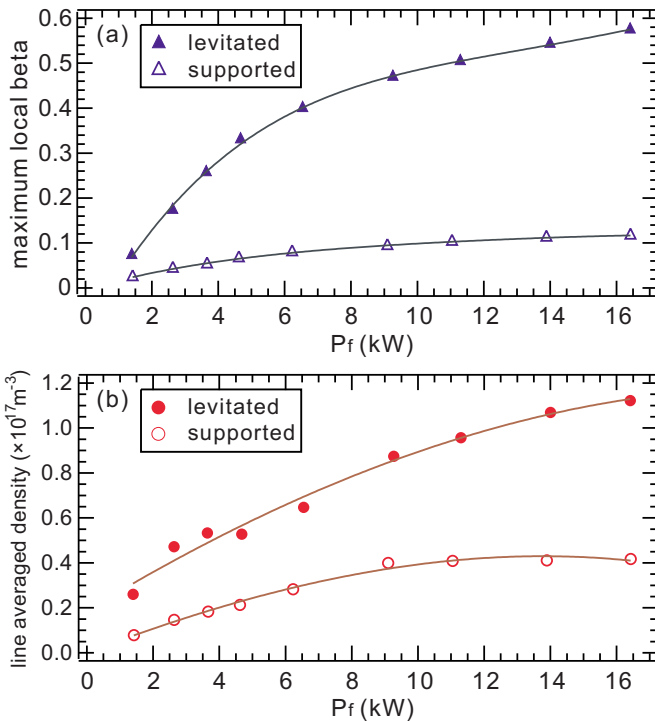


FIG. 2. (Color online) Hot-electron low-density high-beta plasma on RT-1. With levitating the superconducting ring magnet, significant improvement of the confinement is observed in (a) the peak beta (estimated by diamagnetic signals) and (b) the average density (interferometry of microwave transmitted through a horizontal line passing near the magnet). The horizontal axis is the ECH (2.45 GHz) power.

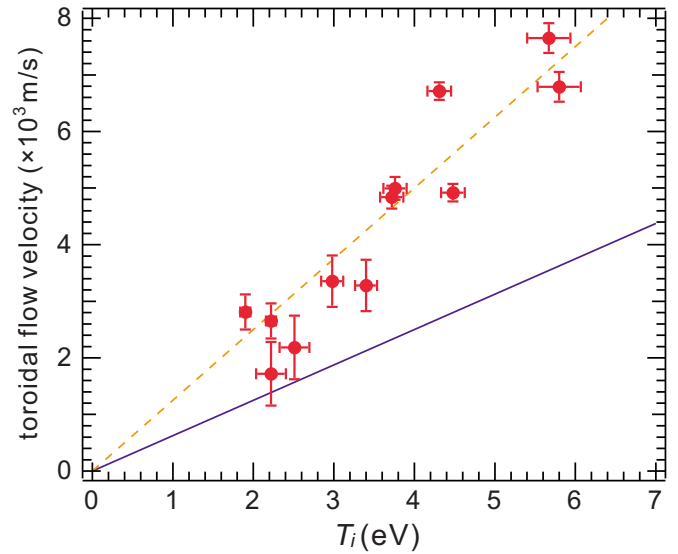


FIG. 3. (Color online) Experimental relation between the ion temperature and the ion flow velocity (in the toroidal direction), which were measured by the spectroscopy of He(II) lines ($\lambda \approx 468.6$ nm); for this experiment, we produced He plasma. In the figure, the solid and dashed lines show the simple estimate of the ion diamagnetic drift velocity $(5/2)T_i/(BL)$ with $B=2 \times 10^{-2}$ T, $L=0.2$ m (solid line) and $L=0.1$ m (dashed line); see Sec. III B.

$$q_j(\widetilde{\mathbf{E}}_j + \mathbf{V}_j \times \widetilde{\mathbf{B}}_j) = 0, \quad (1)$$

where

$$\widetilde{\mathbf{E}}_j = -\partial_t \widetilde{\mathbf{A}}_j - \nabla \widetilde{\phi}, \quad \widetilde{\mathbf{B}}_j = \nabla \times \widetilde{\mathbf{A}}_j, \quad (2)$$

and with the generalized four potentials

$$\widetilde{\phi} = \phi + \frac{1}{q_j} \left(\frac{1}{2} m_j V_j^2 + h_j \right), \quad \widetilde{\mathbf{A}}_j = \mathbf{A} + \frac{m_j}{q_j} \mathbf{V}_j \quad (3)$$

(or $q_j \widetilde{\phi}$ is the effective Hamiltonian, and $q_j \widetilde{\mathbf{A}}_j$ is the canonical momentum). We note that the *generalized electric force* $q_j \widetilde{\mathbf{E}}_j$ includes the kinetic (inertial) and thermal (pressure) forces and the *generalized magnetic force* $q_j \mathbf{V}_j \times \widetilde{\mathbf{B}}_j$ includes

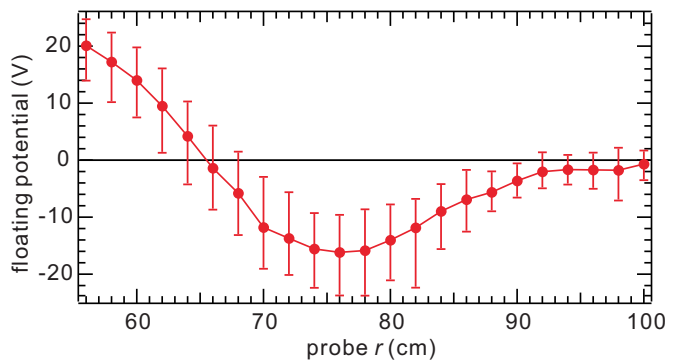


FIG. 4. (Color online) Experimental observation of the internal space potential (measured by an inserted high-impedance Langmuir probe). The measurement is possible only for relatively low temperature plasma (in this measurement, the maximum beta is around 0.003). In a higher beta plasma, we also observe negative potential $\phi = -10$ to -20 V in the peripheral region ($r=80$ – 100 cm), while the potential deeper inside is not directly measurable.

the Coriolis force.⁵ Here we have used a barotropic relation to write $\nabla p_j/n = \nabla h_j$ (p_j : pressure, h_j : molar enthalpy). We assume the ideal equation of state with the internal energy density $n\mathcal{E}_j = p_j/(\gamma-1)$ ($\gamma=5/3$: specific heat ratio).⁶ Then,

$$h_j = \frac{\partial(n\mathcal{E}_j)}{\partial n} = \frac{\gamma}{\gamma-1} \frac{p}{n} = \frac{5}{2} T_j. \quad (4)$$

Note that the generalized electric field, $-q_j \partial_t \widetilde{\mathbf{A}}_j = -q_j \partial_t \mathbf{A} - m_j \partial_t \mathbf{V}_j$, is made up of the induction electric force and the inertia force. In equilibrium states, the solutions to the system (1) with $\partial_t = 0$, the generalized electric field (without the inertia terms) balances the generalized magnetic force.

Simultaneous vanishing of both the generalized electric and magnetic forces,

$$\widetilde{\mathbf{E}}_j = 0, \quad \mathbf{V}_j \times \widetilde{\mathbf{B}}_j = 0, \quad (5)$$

yields a very interesting class of equilibrium solutions of Eq. (1). In Sec. III A, we shall discuss the Bernoulli–Beltrami equilibria defined by these two equations, known, respectively, as Bernoulli and Beltrami conditions.^{7–9} The reader is also referred to Ref. 10 for a wider application of the Bernoulli–Beltrami condition in the theory of diamagnetism.

B. Scale hierarchy

We may delineate the scale hierarchy of the two-fluid system by *normalizing* the variables in Eq. (1). It is convenient to write two different sets of normalized equations, one suited to highlight the ion-inertia scale and the other to do the same for the electron-inertia scale.

The system is normalized in terms of length L_0 (=system size), velocity V_0 , magnetic field B_0 , density n_0 , and a reference energy density $\mathcal{E}_0 = mV_0^2$, where $m = m_i$ (ion mass) for the first set highlighting the ion-inertia regime (see Sec. III A) and $m = m_e$ (electron mass) for the second set pertaining to the electron-inertia regime (see Sec. IV A). The normalized variables are defined by

$$\mathbf{x} = L_0 \hat{\mathbf{x}}, \quad t = (L_0/V_0) \hat{t},$$

$$\mathbf{V}_j = V_0 \widehat{\mathbf{V}}_j, \quad \mathbf{B} = B_0 \widehat{\mathbf{B}}, \quad n = n_0 \widehat{n},$$

$$\mathbf{A} = L_0 B_0 \widehat{\mathbf{A}},$$

$$h_j = \mathcal{E}_0 \widehat{h}_j, \quad e\phi = \mathcal{E}_0 \widehat{\phi},$$

and the frequencies ω_{c_j} (cyclotron frequency) and ω_{p_j} (plasma frequency) will be evaluated at B_0 and n_0 .

For the set pertinent to the ion-inertia regime, we choose $m = m_i$; the two-fluid system (1) then reads (assuming $\partial_t = 0$)

$$\widehat{\nabla} \left(\widehat{\phi} - \widehat{h}_e - \varepsilon \frac{\widehat{V}_e^2}{2} \right) = \widehat{\mathbf{V}}_e \times \left[\widehat{\nabla} \times \left(\frac{\widehat{\mathbf{A}}}{\widehat{\delta}_e} - \varepsilon \widehat{\mathbf{V}}_e \right) \right], \quad (6)$$

$$\widehat{\nabla} \left(\widehat{\phi} + \widehat{h}_i + \frac{\widehat{V}_i^2}{2} \right) = \widehat{\mathbf{V}}_i \times \left[\widehat{\nabla} \times \left(\frac{\widehat{\mathbf{A}}}{\widehat{\delta}_i} + \widehat{\mathbf{V}}_i \right) \right], \quad (7)$$

where

$$\varepsilon = \frac{m_e}{m_i}, \quad \delta_i = \frac{V_0/\omega_{ci}}{L_0}. \quad (8)$$

In this regime, it is often convenient to choose $V_0 = V_A = B_0/\sqrt{\mu_0 m_i n_0}$, the Alfvén speed. Then, $\delta_i = \Delta_i/L_0$ with the ion-inertia length

$$\Delta_i = \frac{V_A}{\omega_{ci}} = \frac{c}{\omega_{pi}} = \sqrt{\frac{m_i}{\mu_0 n e^2}}.$$

The conventional beta ratio (of each species) reads as

$$\beta_j \equiv \frac{p_j}{B^2/(2\mu_0)} = \frac{2\gamma}{\gamma-1} \frac{\widehat{n} \widehat{h}_j}{\widehat{B}^2}. \quad (9)$$

When we study the electron-inertia regime, equilibrium equations become more transparent with the choice $m = m_e$. The appropriate normalized equations, in the new normalized variables, are (now marked by “check”)

$$\check{\nabla} \left(\check{\phi} - \check{h}_e - \frac{\check{V}_e^2}{2} \right) = \check{\mathbf{V}}_e \times \left[\check{\nabla} \times \left(\frac{\check{\mathbf{A}}}{\check{\delta}_e} - \check{\mathbf{V}}_e \right) \right], \quad (10)$$

$$\check{\nabla} \left(\check{\phi} + \check{h}_i + \varepsilon^{-1} \frac{\check{V}_i^2}{2} \right) = \check{\mathbf{V}}_i \times \left[\check{\nabla} \times \left(\frac{\check{\mathbf{A}}}{\check{\delta}_e} + \varepsilon^{-1} \check{\mathbf{V}}_i \right) \right], \quad (11)$$

where

$$\check{\delta}_e = \frac{V_0/\omega_{ce}}{L_0}. \quad (12)$$

In Sec. IV, we will choose $V_0 = c$ to study the electron-inertia regime.

III. SPONTANEOUS ION FLOW

A. Ion-inertia (Hall MHD) regime

The study of the ion-inertia regime can be effectively conducted in the Hall MHD model obtained by neglecting the electron-inertia ($\varepsilon=0$) in systems (6) and (7). Conventional Hall MHD system is obtained by the replacement $\mathbf{V}_e = \mathbf{V}_i - \mathbf{j}/(en)$ where the electric current density $\mathbf{j} = \mu_0^{-1} \nabla \times \mathbf{B}$ when the displacement current is neglected. The equilibrium conditions (6) and (7) reduce to

$$\widehat{\nabla} \left(\widehat{\phi} - \widehat{h}_e \right) = \left(\frac{\widehat{\mathbf{V}}_i}{\widehat{\delta}_i} - \frac{\widehat{\nabla} \times \widehat{\mathbf{B}}}{\widehat{n}} \right) \times \widehat{\mathbf{B}}, \quad (13)$$

$$\widehat{\nabla} \left(\widehat{\phi} + \widehat{h}_i + \frac{\widehat{V}_i^2}{2} \right) = \widehat{\mathbf{V}}_i \times \left(\frac{\widehat{\mathbf{B}}}{\widehat{\delta}_i} + \widehat{\nabla} \times \widehat{\mathbf{V}}_i \right). \quad (14)$$

MHD (scale-free) limit. In the limit of $\delta_i \rightarrow 0$, the term of order δ_i^{-1} yields

$$\widehat{\mathbf{V}}_i \times \widehat{\mathbf{B}} = 0,$$

implying that the static ion flow, if any, must be aligned with the magnetic field.¹¹ Subtracting Eq. (13) from Eq. (14), we obtain the standard MHD equilibrium equation

$$\widehat{\nabla} \left(\widehat{h}_e + \widehat{h}_i + \frac{\widehat{V}_i^2}{2} \right) = \frac{\widehat{\nabla} \times \widehat{\mathbf{B}}}{\widehat{n}} \times \widehat{\mathbf{B}} + \widehat{\mathbf{V}}_i \times (\widehat{\nabla} \times \widehat{\mathbf{V}}_i). \quad (15)$$

In a flow-free equilibrium ($\widehat{\mathbf{V}}_i=0$), the ion Eq. (14) demands the ion pressure to be balanced only by the electric potential, i.e., $\widehat{\phi} + \widehat{h}_i = 0$ so that the ions are confined by the electric potential [then Eq. (13) reduces to the ion Bernoulli condition $\widehat{\mathbf{E}}_i=0$]. The electric field transfers the ion pressure to the electrons, and the total pressure is balanced by the Lorentz force on the electrons.

Ion-inertia regime. If $\delta_i \geq 1$, the ion flow $\widehat{\mathbf{V}}_i$ and the potential $\widehat{\phi}$ are not forced to degenerate into the aforementioned MHD equilibrium, but have the potential to create diverse structures. By Eq. (14), $\widehat{\mathbf{V}}_i$ must be at least of order $\delta_i(\widehat{\phi} + \widehat{h}_i)$. Unlike the MHD limit, $\widehat{\phi}$ is freed from \widehat{h}_i . If $\widehat{\phi} \sim 0$ (more precisely, $\widehat{\nabla} \widehat{\phi} \sim 0$), $\widehat{\mathbf{V}}_i \sim \delta_i \widehat{h}_i \sim \delta_i \beta_i$ [see Eq. (9)]. We will attempt to show, in Sec. III B, that the low-density RT-1 plasma is in this regime.

If $\delta_i \beta_i$ is of order 1, the ion Eq. (14) becomes nonlinear with respect to $\widehat{\mathbf{V}}_i$, and, then, a variety of interesting structures may be sustained.^{2,12} The ultimate relaxed (but nontrivial) equilibria will satisfy the Bernoulli–Beltrami conditions by both ions and electrons,^{7–9} i.e., the gradient and the nongradient forces in the electron and ion Eqs. (13) and (14) vanish independently,

$$\widehat{\phi} - \widehat{h}_e = 0, \quad (\widehat{\mathbf{V}}_i - \delta_i \widehat{\nabla} \times \widehat{\mathbf{B}}/\widehat{n}) \times \widehat{\mathbf{B}} = 0,$$

$$\widehat{\phi} + \widehat{h}_i + \widehat{V}_i^2/2 = 0, \quad \widehat{\mathbf{V}}_i \times (\widehat{\mathbf{B}} + \delta_i \widehat{\nabla} \times \widehat{\mathbf{V}}_i) = 0.$$

Note that this solution has a finite $\widehat{\mathbf{V}}_i$, generalizing the previous degenerate ion Bernoulli condition.

We also note that the *Taylor relaxed state*¹³ is the realization of the electron Bernoulli–Beltrami conditions ($\widehat{\mathbf{E}}_e=0$ and $\widehat{\mathbf{V}}_e \times \widehat{\mathbf{B}}_e \approx \widehat{\mathbf{V}}_e \times \widehat{\mathbf{B}}=0$) with the degenerate ion Bernoulli–Beltrami conditions ($\widehat{\mathbf{E}}_i=0$ and $\widehat{\mathbf{V}}_i=0$).¹⁴ This configuration does not confine the plasma, i.e., the magnetic field exerts no force on the plasma.

B. Experimental observation in the ion-inertia range

As described in the Introduction, the RT-1 plasma, operating at low-density ($\leq 10^{17} \text{ m}^{-3}$), is characterized by large h_e ($\leq 10^{-14} \text{ J}$), small h_i ($\leq 10^{-17} \text{ J}$), and small $e\phi$ ($\leq 10^{-17} \text{ J}$). The ion-inertia length Δ_i is about 1 m, which is longer than the characteristic length scale of the pressure gradient ($L_0=0.05\text{--}0.2 \text{ m}$). Thus, the scaling parameter $\delta_i=5\text{--}20$, implying that the ion-inertia range determines the global structure.

Figure 3 shows the spectroscopic measurements of the ion temperature and the toroidal (azimuthal) ion flow velocity near the center of the confinement region (major radius $\approx 0.6 \text{ m}$, where $B \approx 2 \times 10^{-2} \text{ T}$; see Fig. 1). We find that V_i (in the direction perpendicular to \mathbf{B}) is approximately proportional to T_i . We may analyze the ion Eq. (14) as follows. Since $\widehat{\mathbf{V}}_i$ is small, we may neglect the nonlinear terms and

estimate $\widehat{\mathbf{V}}_i \approx \delta_i(\widehat{\phi} + \widehat{h}_i)$ with the appropriate choices of L_0 and B_0 . Translating back to physical units, we obtain a familiar expression,

$$V_i [\text{m/s}] \approx \frac{\phi [\text{V}] + (5/2)T_i [\text{eV}]}{B [\text{T}] \times L [\text{m}]},$$

where L is the length scale of the local gradient. In Fig. 3, the solid and dashed lines show the *diamagnetic drift* velocity $(5/2)T_i/(BL)$ with $B=2 \times 10^{-2} \text{ T}$, $L=0.2 \text{ m}$ (solid line), and $L=0.1 \text{ m}$ (dashed line). For the vacuum magnetic field, $B/|\nabla B|$ is approximately 0.2 m. The pressure has a steeper gradient. By fitting multichannel magnetic measurements, we typically have $L \approx 0.1 \text{ m}$.

The electric field also makes same-order contribution to the ion flow (so-called $\mathbf{E} \times \mathbf{B}$ drift). As shown in Fig. 4, the potential has a nonmonotonic profile, yielding a complicated drive of the flow. The point is that $\widehat{\phi}$ does not balance \widehat{h}_i and cancel V_i (as the ideal MHD model demands); their decoupling allows the emergence of $\widehat{\mathbf{V}}_i$ of the order of $\delta_i \widehat{h}_i$.

In this parameter range, the nonlinear terms [$\widehat{\nabla}(\widehat{V}_i^2/2)$ and $\widehat{\mathbf{V}}_i \times (\widehat{\nabla} \times \widehat{\mathbf{V}}_i)$] in the ion equation are negligible. However, $\widehat{\mathbf{V}}_i$ approaches 1 (i.e., V_i reaches the Alfvén speed) if $\widehat{h}_i \sim \beta_i$ becomes of the order of $\delta_i^{-1} \sim 0.1$, and then the nonlinear terms become comparable to the linear terms (see Refs. 15 and 16 for experimental observations of rapidly rotating plasmas and also Ref. 17 for theoretical examination of the two-fluid effect in the pedestal of the pressure profile).

The electron equilibrium condition is more nontrivial. For negligible $\widehat{\phi}$ and $\widehat{\mathbf{V}}_i/\delta_i$, the electron Eq. (13) reduces to the standard MHD equilibrium equation (with negligible ion enthalpy). However, the neglect of the electron-inertia may not be always appropriate. In the next section, we will investigate the electron-inertia effect and show that interesting new equilibria stem when Eq. (13) is corrected for electron-inertia.

IV. HOT ELECTRON CONFINEMENT

A. Equilibrium condition in the electron-inertia regime

In the hot electron low-density regime, we may not neglect the electron-inertia. To study this regime, we will use the electron equilibrium Eq. (10) with the choice $V_0=c$ and $L_0=\Delta_e=c/\omega_{pe}$. The unit energy density is $m_e c^2$ ($\approx 0.5 \text{ MeV}$), by which we normalize $e\phi$ and h_e . Then, Eq. (10) may be rewritten as

$$\check{\nabla} \left(\check{\phi} - \check{h}_e - \frac{\check{V}_e^2}{2} \right) - \check{\mathbf{V}}_e \times \left[\left(\frac{\omega_{ce}}{\omega_{pe}} \right) \mathbf{B} - \check{\nabla} \times \check{\mathbf{V}}_e \right] = 0. \quad (16)$$

In this context, Ampere's law, neglecting the ion current, takes the form

$$\left(\frac{\omega_{ce}}{\omega_{pe}} \right) \check{\nabla} \times \check{\mathbf{B}} = -\check{n} \check{\mathbf{V}}_e. \quad (17)$$

For the plasma parameters relevant to the RT-1 experiments, we estimate $\check{h}_e \geq 0.01$ and the scaling parameter $\omega_{ce}/\omega_{pe} \approx 0.1$. To satisfy Eq. (16), then, we need \check{V}_e of order

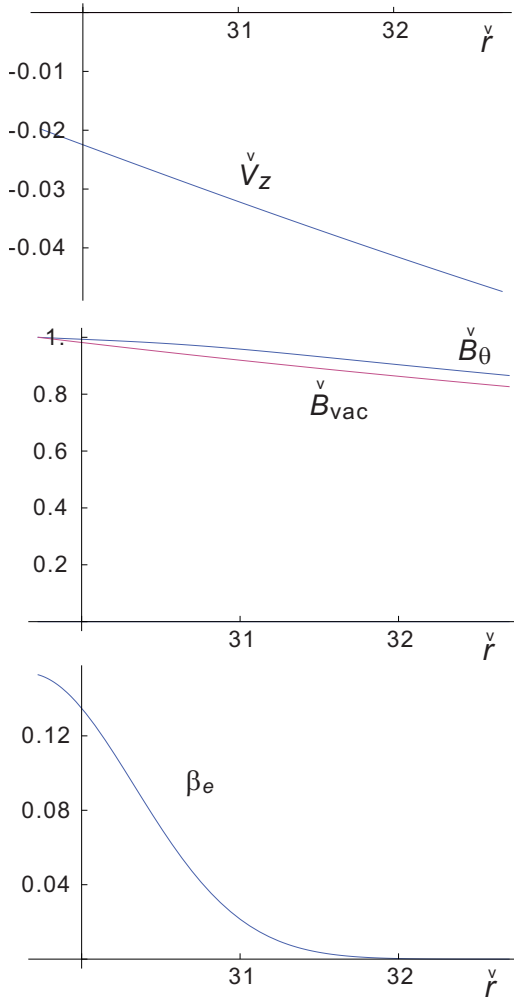


FIG. 5. (Color online) Electron diamagnetic equilibrium ($\mu=0$, $\alpha=0.9$). The diamagnetic electron current modifies \check{B}_θ from the vacuum magnetic field \check{B}_{vac} .

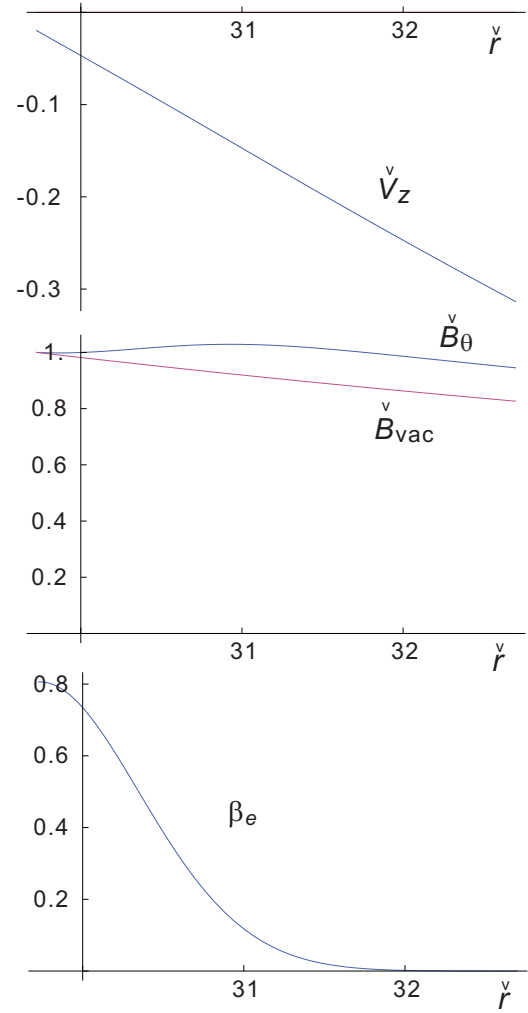


FIG. 6. (Color online) Ultra-high-beta electron Bernoulli-Beltrami equilibrium ($\mu=0$, $\alpha=0$). When $\mu=0$, the electron vorticity cancels the magnetic field to make the effective (generalized) magnetic field zero. Such a field structure is strongly diamagnetic and confines very high-beta electrons.

0.1; evidently the kinetic pressure term ($\check{\nabla} \check{V}_e^2/2$) and the vorticity term [$\check{\nabla}_e \times (\check{\nabla} \times \check{V}_e)$] are comparable to the thermal pressure ($\check{\nabla} \check{h}_e$) and the magnetic [$(\omega_{ce}/\omega_{pe}) \check{V}_e \times \check{\mathbf{B}}$] terms.

We will now explore different solutions of Eqs. (16) and (17). We find that the *electron Bernoulli-Beltrami* solution can show extreme diamagnetism, that is, the plasma can sustain very large pressure gradients.

B. Generalized Bernoulli-Beltrami equilibria

As described in Sec. II A, the Bernoulli-Beltrami equilibrium pertains when both terms of equilibrium condition (16) independently vanish,

$$\check{\nabla} \left(\check{\phi} - \check{h}_e - \frac{\check{V}_e^2}{2} \right) = 0, \quad (18)$$

$$\check{\nabla}_e \times \left[\left(\frac{\omega_{ce}}{\omega_{pe}} \right) \check{\mathbf{B}} - \check{\nabla} \times \check{V}_e \right] = 0. \quad (19)$$

The Beltrami condition (19) is equivalent to

$$\left(\frac{\omega_{ce}}{\omega_{pe}} \right) \check{\mathbf{B}} - \check{\nabla} \times \check{V}_e = \mu \check{V}_e, \quad (20)$$

where μ is a scalar function such that $\check{\nabla} \cdot (\mu \check{V}_e) = 0$ (the divergence of $\check{\mathbf{B}}$ must be zero). By weakening the complete alignment of the current $-\check{V}_e$ and the generalized magnetic field $(\omega_{ce}/\omega_{pe}) \check{\mathbf{B}} - \check{\nabla} \times \check{V}_e$, we may generalize Eq. (20) to encompass broader classes of equilibria; here we put

$$\left(\frac{\omega_{ce}}{\omega_{pe}} \right) \check{\mathbf{B}} - \check{\nabla} \times \check{V}_e = \mu \check{V}_e + \alpha \left(\frac{\omega_{ce}}{\omega_{pe}} \right) \check{\mathbf{B}}. \quad (21)$$

Then the equilibrium condition (16) reads as

$$\check{\nabla} \left(\check{\phi} - \check{h}_e - \frac{\check{V}_e^2}{2} \right) - \alpha \left(\frac{\omega_{ce}}{\omega_{pe}} \right) \check{V}_e \times \check{\mathbf{B}} = 0. \quad (22)$$

We comment on the generality/specialty of the equilibrium condition (22). In the general equilibrium Eq. (16), the vector [$(\omega_{ce}/\omega_{pe}) \check{\mathbf{B}} - \check{\nabla} \times \check{V}_e$] is divergence-free, thus it can be represented by two scalar functions. We may regard that μ and α in Eq. (21) correspond to these two degrees of

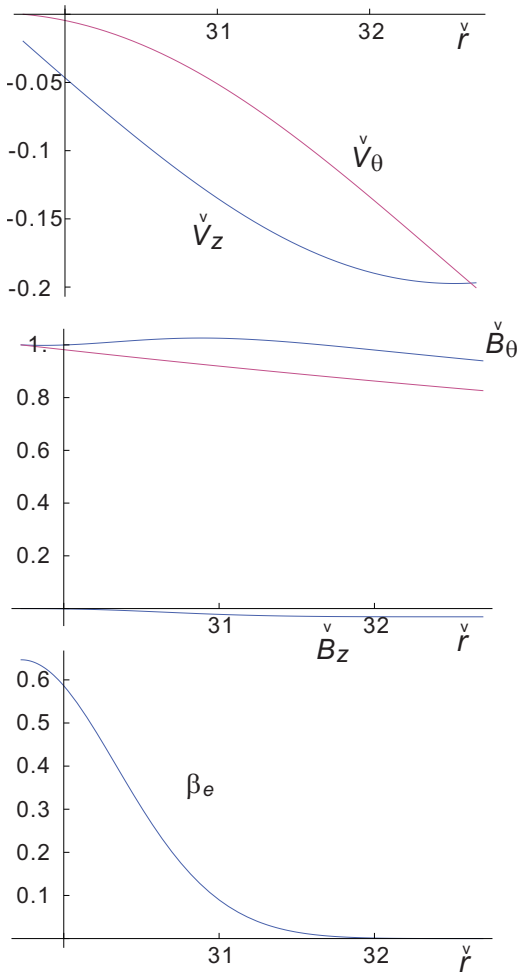


FIG. 7. (Color online) High-beta electron Bernoulli–Beltrami equilibrium ($\mu=0.5$, $\alpha=0$). A finite μ produces couplings between \check{B}_θ and \check{B}_z or \check{V}_θ and \check{V}_z , producing a “spiral” structure.

freedom, if $\check{\mathbf{B}}$ and $\check{\mathbf{V}}_e$ are not parallel.¹⁸ The parallel case is, indeed, not included in Eq. (22), but it is not relevant here; we do not observe an appreciable parallel current $-\check{n}\check{\mathbf{V}}_e \parallel \check{\mathbf{B}}$ that will produce a toroidal magnetic field.

C. Cylindrical-geometry solutions

In this subsection, we solve Eqs. (17), (21), and (22) for an axisymmetric system assuming μ and α to be constants. Denoting $\check{\mathbf{B}} = (\omega_{ce}/\omega_{pe})\check{\mathbf{B}}$, the determining equations are (in r - θ - z cylindrical coordinates)

$$\partial_r \check{V}_{ez} = -(1 - \alpha)\check{B}_\theta - \mu\check{V}_{e\theta},$$

$$\partial_r \check{V}_{e\theta} + r^{-1}\check{V}_{e\theta} = (1 - \alpha)\check{B}_z + \mu\check{V}_{ez},$$

$$\partial_r \check{B}_z = \check{n}\check{V}_{e\theta},$$

$$\partial_r \check{B}_\theta + \nu r^{-1}\check{B}_\theta = -\check{n}\check{V}_{ez},$$

$$\partial_r [\check{h}_e + (\check{V}_{ez}^2 + \check{V}_{e\theta}^2)/2] = \alpha(\check{V}_{ez}\check{B}_\theta - \check{V}_{e\theta}\check{B}_z),$$

where ν is a positive constant that controls the geometric decay of the magnetic field (if $\nu=2$, $B \propto r^{-2}$ simulating the dipole magnetic field). We have omitted $\check{\phi}$ which is negligible in comparison with \check{h}_e (so the ion equation is decoupled from the electron equation).

The region near the plasma edge ($r \gtrsim 0.5$ m) is the subject of interest. For typical parameters, we calculate $\Delta_e \sim 0.02$ m ($n_0 \sim 10^{17}$ m⁻³) and $\omega_{ce}/\omega_{pe} \sim 0.1$. The density $\check{n}(r)$ is assumed to be a rapidly decreasing function,

$$\check{n}(r) = \check{n}_{\text{edge}} \exp[-(r - r_{\text{edge}})^2],$$

where we put $\check{n}_{\text{edge}}=0.2$ and $r_{\text{edge}}=0.5/\Delta_e$.

In Fig. 5, we show a relatively conventional diamagnetic solution (with $\alpha=0.9$ and $\mu=0$). The electron pressure is primarily balanced by the *generalized* Lorentz force (including the *Coriolis* force produced by electron vorticity) due to the toroidal electron flow (current) $\check{V}_{e\theta}$ and the generalized poloidal magnetic field $\alpha\hat{B}_\theta$.

When $\alpha=0$, the generalized Lorentz force vanishes (Beltrami condition), and, then, the electron pressure is confined purely by the *hydrodynamic pressure* contributed by $\check{V}_e^2/2$ (Bernoulli condition). As shown in Fig. 6, such a Bernoulli–Beltrami equilibrium has very strong diamagnetism.

A finite μ produces couplings between the poloidal and toroidal components of the magnetic field and flow, producing a spiral structure. In Fig. 7, we show a solution with $\mu=0.5$ and $\alpha=0$.

V. SUMMARY

We have made an attempt to understand and interpret the observed properties of high-beta hot electron plasma produced on the RT-1 magnetospheric device in terms of the equilibria accessible to the generalized two-fluid electron-ion plasma. Because of low-density, the ion-inertia length is comparable to (or larger than) the macroscopic system size. Hence, the ion and electron motions are easily decoupled. Static equilibrium models no longer apply; the ion diamagnetism causes strong ion flow. Because of the low ion temperature, the ion flow is still in the *linear regime*, i.e., the hydrodynamic pressure or the vorticity effect (Coriolis force) of the ion flow (which are expressed as quadratic terms) are negligible. Based on the present analysis, however, we expect that nonlinear structures (approaching to the Bernoulli–Beltrami state) will emerge when $\beta_i \gtrsim 0.1$.

On the other hand, electrons may create structures in the smaller scale hierarchy dictated by the electron-inertia length. The low-density, low magnetic field edge region sets the stage for this new creation. Here again we expect that the nonlinear hydrodynamic pressure and vorticity will play an interesting role; the Bernoulli–Beltrami state can confine very high-beta plasmas creating a pedestal-like steep pressure gradient near the plasma edge.

ACKNOWLEDGMENTS

We acknowledge the support given by the RT-1 project members. This work was supported by Grants-in-Aid for Scientific Research (Grant No. 19340170) from MEXT, Japan.

¹S. M. Mahajan, *Phys. Rev. Lett.* **90**, 035001 (2003).

²Z. Yoshida, S. M. Mahajan, and S. Ohsaki, *Phys. Plasmas* **11**, 3660 (2004).

³The RT-1 device is a “laboratory magnetosphere” which confines a plasma in a dipole magnetic field produced by a levitating superconducting magnet, see Z. Yoshida, Y. Ogawa, J. Morikawa, S. Watanabe, Y. Yano, S. Mizumaki, T. Tosaka, Y. Ohtani, A. Hayakawa, and M. Shibui, *J. Plasma Fusion Res.* **1**, 008 (2006); Z. Yoshida, Y. Ogawa, J. Morikawa, M. Furukawa, H. Saitoh, M. Hirota, D. Hori, J. Shiraishi, S. Watanabe, S. Numazawa, Y. Yano, and J. Suzuki, *Fusion Sci. Technol.* **51**, 29 (2007); Z. Yoshida, H. Saitoh, J. Morikawa, Y. Yano, S. Watanabe, and Y. Ogawa, *Phys. Rev. Lett.* **104**, 235004 (2010).

⁴D. T. Garnier, A. C. Boxer, J. L. Ellsworth, J. Kesner, and M. E. Mauel, *Nucl. Fusion* **49**, 055023 (2009).

⁵Here we ignore the ion viscosity with respect to the ion-inertia term (and the electromagnetic and pressure terms). It is well known that any compressible flow will be strongly damped by the so-called “parallel viscosity” which is $(V_{th}/V_i)(L_c/L)$ (L_c is the mean free path) times larger than the inertia term. For incompressible flows, however, the relevant viscous damping of the shear flows is, by a factor ρ/L_c (ρ is the ion gyroradius), smaller than the parallel viscosity. Consequently for the incompressible “Beltrami flows” (Ref. 2), considered in this paper, the viscous damping term may be negligible (compared to the inertial term) for an appreciably large ion flow velocity.

⁶Assuming the ideal state equation, the internal energy density can be written as $n\mathcal{E}=C_V T$ with the temperature T and the specific heat

$C_V=nk_B/(\gamma-1)$. The enthalpy is, then, $nh=\gamma C_V T=nk_B T\gamma/(\gamma-1)=p\gamma/(\gamma-1)$. Defining $V_{th}=\sqrt{k_B T/m}$, we can write $h=mV_{th}^2\gamma/(\gamma-1)$.

⁷L. C. Steinhauer and A. Ishida, *Phys. Rev. Lett.* **79**, 3423 (1997).

⁸S. M. Mahajan and Z. Yoshida, *Phys. Rev. Lett.* **81**, 4863 (1998).

⁹Z. Yoshida and S. M. Mahajan, *Phys. Rev. Lett.* **88**, 095001 (2002).

¹⁰S. M. Mahajan, *Phys. Rev. Lett.* **100**, 075001 (2008).

¹¹It is remarked that we are considering only static flows; time-dependent ion flows are primarily caused by the component $-\partial_t \mathbf{A}$ of the electric field which scales as $V_0 B_0 = \mathcal{E}_0 / (e\Delta_i)$, thus can balance with $\widehat{\mathbf{V}}_i \times \widehat{\mathbf{B}}$, resulting in the $\mathbf{E} \times \mathbf{B}$ drift perpendicular to the magnetic field. In contrast, the static flows, caused by the $-\nabla\phi$ part of the electric field and scaling as $\mathcal{E}_0 / (eL_0)$, obey the so-called drift-ordering with characteristic velocity on the order of the ion diamagnetic drift velocity.

¹²G. N. Throumoulopoulos and H. Tasso, *Phys. Plasmas* **13**, 102504 (2006).

¹³J. B. Taylor, *Phys. Rev. Lett.* **33**, 1139 (1974).

¹⁴The Taylor relaxed state is characterized as the minimizer of the magnetic field energy $E = \int (B^2/2) dx$ for a given magnetic helicity $H = \int \mathbf{B} \cdot \mathbf{A} dx$. Adding the fluid kinetic energy $\int (V^2/2) dx$ to E and restricting also the cross helicity $K = \int \mathbf{B} \cdot \mathbf{V} dx$, we obtain a generalized Taylor state which contains a parallel flow, see R. N. Sudan, *Phys. Rev. Lett.* **42**, 1277 (1979); K. Avinash and J. B. Taylor, *Comments Plasma Phys. Controlled Fusion* **14**, 127 (1991).

¹⁵H. Y. Guo, A. L. Hoffman, L. C. Steinhauer, K. E. Miller, and R. D. Milroy, *Phys. Rev. Lett.* **97**, 235002 (2006).

¹⁶T. Kanki and M. Nagata, *Phys. Plasmas* **13**, 072506 (2006).

¹⁷P. N. Guzdar, S. M. Mahajan, and Z. Yoshida, *Phys. Plasmas* **12**, 032502 (2005).

¹⁸To be precise, μ and α are the *Cauchy characteristic functions* corresponding to the two hyperbolic parts of the system of partial differential Eqs. (16) and (17). Together with $\nabla \cdot \check{\mathbf{B}} = 0$, these constitute five-elliptic and two-hyperbolic system that demands two Cauchy characteristic functions for integration (the characteristics are the streamlines of $\check{\mathbf{V}}_c$).